Raman and Vibronic Spectra of the Nitrite Ion in Alkali Halides†

A. R. Evans* and D. B. Fitchen
Laboratory of Atomic and Solid State Physics, Cornell University, Ithaca, New York 14850
(Received 24 March 1970)

Raman and vibronic absorption spectra associated with NO_2^- substitutional impurity in KCl, KBr, KI, and NaBr at 6 °K are reported. The equilibrium orientation of the nitrite ion at low temperatures is determined from the stress-induced dichroism or splitting of the vibronic lines. Rotational fine structure on these lines is analyzed in terms of hindered rotation of the nitrite ion. Structure at higher frequencies in the vibronic and Raman spectra is assigned to perturbed lattice modes.

I. INTRODUCTION

The motion of a substitutional impurity atom and its effect on the lattice dynamics of its host crystal have been the subject of renewed experimental and theoretical interest. If the impurity itself is anisotropic, as for instance a molecular impurity, then the interaction with the host lattice is more complex. In particular, the motions of the impurity will conclude libration, hindered rotation, or free rotation, depending on the strength of the anisotropic crystal potential. Recently, there has been some success in understanding this more complicated behavior.[1–3]

The present study originated from a survey of impurity-induced Raman spectra in alkali halides. Much work has been done on the absorption spectra of NO_2^- ions in alkali halides to investigate the vibrational and librational modes of this substitutional impurity. NO_2^- was chosen for the Raman study to see how these motions might affect the spectra. Pure alkali halides do not show first-order Raman scattering, but the inclusion of the defect destroys inversion symmetry for the neighboring ions and gives rise to a first-order Raman spectrum characteristic of the perturbed vibrations of these ions.

In the course of the study, we have also investigated the fine structure of the uv absorption band of molecule. Some of this structure is characteristic of the perturbed lattice vibrations, and has been reported before by Timusk and Staude.[4] Still finer rotational structure is also observed in some cases, and we have analyzed this to determine the rotational behavior of the molecule in the excited electronic state. Finally, we have made preliminary measurements on samples where the NO_2^- molecules were oriented under uniaxial stress at low temperatures.

II. EXPERIMENTAL TECHNIQUES

A. Sample Preparation

Nitrite-doped crystals of KCl, KBr, KI, and NaBr were grown at Cornell by the Kyropoulos technique following purification procedures described by Pohl.[5] Dopings of the appropriate alkali nitrite powder in the melt ranged from 0.3 to 3 mole %. The actual NO_2^- concentrations in the samples used were determined by colorimetric analysis and ranged from 0.02 to 2.0 mole %. Near- and far-infrared spectra and the measurements to be reported here suggest that the optically active NO_2^- ions are present as isolated impurities.

The concentration of nitrate ion, the most likely other impurity in the samples, was measured by near-infrared spectroscopy and found to be at least an order of magnitude below the nitrite concentration. No evidence of NO_3^- (or other impurities) was found in the recent far-infrared spectrum measured for one of our samples of $KI:NO_2^-$ by Hughes.[6]

Sample stock was cleaved from portions of the boules of high optical quality. Samples were cleaved or ground and polished to dimensions of approximately $2\times3\times10$ mm with the long axis in either the [100] or [110] direction.

B. Raman Spectrometer

The Raman scattering measurements were made using a homemade cw argon-ion laser operating on 4880 Å at a power output of ~50 mW. The polarized and filtered output was focused on the sample mounted in a conduction cryostat. The scattered light at 90° passed through a polaroid analyzer into a Spex 1400 double monochromator, to a cooled EMI 6256S photomultiplier tube. The detector output went to a pulse discriminator and then to a scaler or a storage capacitor. A modified scanning mechanism was used to advance the monochromator wavelength setting in discrete steps of 0.1 or 1.0 Å, and then to count photons at that setting for a preset time interval (usually 10 sec) before advancing to the next setting. The best resolution of the instrument in this experiment was ~2 cm^{-1}, as determined by scanning

laser lines. The accuracy of the wavelength calibration was checked by observing nonlasing argon transitions and by measuring the pattern of white-light interference fringes produced by a fixed-separation Fabry-Perot interferometer.

C. uv Spectra

The vibronic absorption spectra in the near uv were recorded in conduction or immersion helium cryostats in a Cary 14 spectrophotometer. Occasionally, higher resolution (~ 1 cm^{-1}) was achieved using a $\frac{1}{2}$-m Jarrell-Ash scanning monochromator or a 2-m Bausch and Lomb spectrograph.

Temperature dependence of the fine structure was investigated between 1.5 and 4.2 °K by pumping on the helium in the immersion cyrostat.

The effect of uniaxial stress on the spectra was measured with a piston and anvil sample mount in the immersion cryostat. Force was transmitted by concentric thin-wall stainless-steel tubes connected to a hydraulic cylinder. Stresses of up to 8 kg/mm^2 were applied to ⟨100⟩ or ⟨110⟩ oriented crystals at ~ 2 °K before fracture. Spectra, polarized parallel and perpendicular to the stress axis, were recorded.

III. SPECTRA

A. Raman Spectra

Raman spectra were measured at 300, 80, and 6 °K in nitrite-doped KCl, KBr, KI, and NaBr. The impurity-induced spectra observed consist of features in the range of the internal vibration frequencies of the nitrite molecule and in the range of the phonon frequencies of the host lattice.

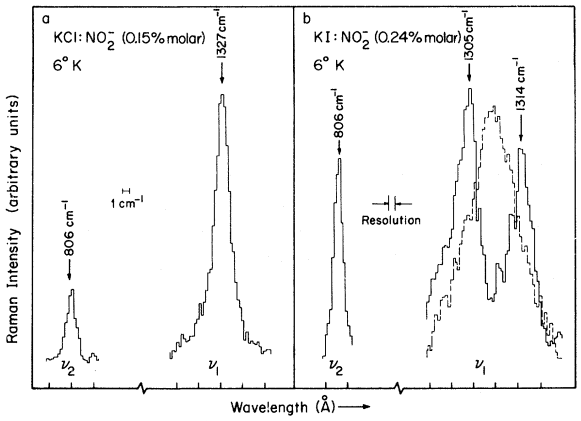

FIG. 1. Raman spectra of two of the internal vibrations of NO_2^-. Unpolarized spectra excited at 4880 Å. The ν_2 line corresponds to the bending mode; ν_1 to the symmetric stretching mode. The dashed curve for KI shows the ν_1 spectrum at 77 °K.

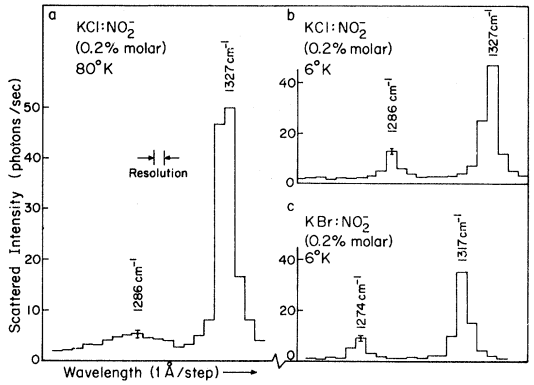

FIG. 2. Raman scattering by the asymmetric stretching mode and the symmetric stretching mode of the nitrite ion.

Relatively sharp lines, corresponding to the bending and symmetric stretching modes of the molecule, were observed at ~ 800 and ~ 1320 cm^{-1}, respectively (Fig. 1). The bending mode line is relatively narrow at all temperatures, whereas the stretching mode line broadens with increasing temperature. The line corresponding to the asymmetric stretching mode is also narrow at 6 °K but is drastically broadened at 80 °K and was not observed at 300 °K (Fig. 2). No lines corresponding to combinations of vibrational modes were observed. Except for the appearance of the 9 cm^{-1} doublet in KI, no fine structure or satellite was observed with these internal vibrational lines. The width and positions of the lines observed are listed in Table I.

The second feature of the Raman scattering is the structure in the range of phonon frequencies. At room temperature this is dominated by second-order bulk Raman scattering, but at 6 °K the latter is greatly reduced and the impurity-induced structure dominates. For most crystals at 6 °K, the bulk scattering contributes about half the background observed in the single-phonon frequency region; the remainder is due to dark counts, the tail of the Rayleigh peak, or stray light entering the monochromator. The impurity-induced Raman spectra are shown for each crystal in Fig. 3. The major peaks are comparable in intensity to the internal-stretching-mode Raman line. The spectrum of a pure KBr crystal at 6 °K is also shown for comparison.

These Stokes spectra were measured for the different polarizations and orientations listed in Table II. These spectra are shown in Fig. 4 for KI, which has the most prominent impurity-induced structure.

An unpolarized spectrum of KI:NO_2^- taken at highest sensitivity is also shown in Fig. 5. This

TABLE I. Internal vibrational modes measured in Raman scattering. Figures in brackets indicate linewidths.

		300 °K (cm^{-1})	80 °K (cm^{-1})	6 °K (cm^{-1})
KCl:NO_2^-	ν_1	1327	1327	1327
		(~15)	(5)	(3)
	ν_2	811	807	806
		(3)	(3)	(3)
	ν_3	...	1286	1286
			(~35)	(~2)
KBr:NO_2^-	ν_1	1317	1317	1317
		(~10)	(5)	(3)
	ν_2	806	801	800
		(4)	(4)	(3)
	ν_3	...	1274	1274
			(≳50)	(3)
				1305
				(~4)
KI:NO_2^-	ν_1	1309	1309	1314
		(~25)	(~8)	(~4)
	ν_2	803	806	806
		(3)	(3)	(~2)
	ν_3	...	...	...
NaBr:NO_2^-	ν_1	...	...	1327
				(4)
	ν_2	...	...	828
				(4)
	ν_3	...	...	~1283
				(~10)

spectrum was taken with laser excitation of 250 mW at 4880 Å. Polarization measurements were not made on the additional weak features shown.

Both types of Raman spectra appeared to scale in intensity with NO_2^- concentration and to be independent of concentration in their shape. The width and position of the sharp features did not vary appreciably in the concentration range ~0.02–1.0%. No additional fine structure on the sharp features could be resolved with our instrumental resolution of ~2 cm^{-1}.

For KI crystals with the heaviest doping, some of the broad phonon peaks showed different relative intensities and positions, and an additional peak at 25 cm^{-1} was reported.[7] This peak does not appear at lower concentrations, so one must presume that it is not due to isolated NO_2^- ions.

Because it is important for the later analysis of the Raman spectra, a test was made of the dependence of Raman intensity on frequency of the exciting laser light. Relative intensity measurements were made on the 76-cm^{-1} gap mode in KI:NO_2^- with the 4579, 4880, and 5145-Å lines

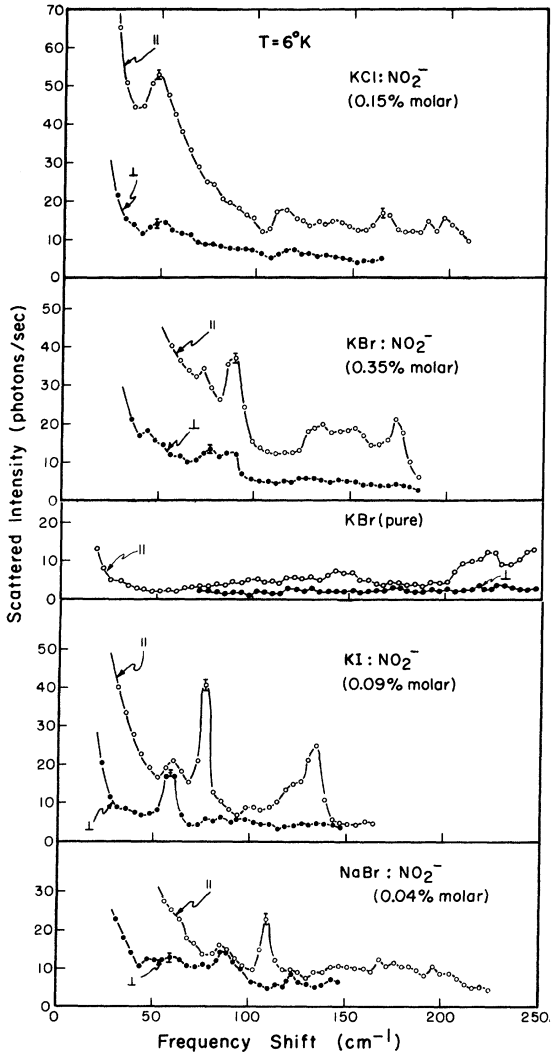

FIG. 3. Low-frequency Raman spectra of NO_2^- at 6 °K. Spectra were measured for polarizations parallel and perpendicular to the [100] polarization of the 4880-Å incident light.

TABLE II. Scattering geometries used to measure polarized spectra.

	$\lvert\alpha_1\rvert^2+\frac{4}{3}\lvert\alpha_{12}\rvert^2$	$\lvert\alpha_{25'}\rvert^2$	$\lvert\alpha_1\rvert^2+\frac{1}{3}\lvert\alpha_{12}\rvert^2+\lvert\alpha_{25'}\rvert^2$	$\lvert\alpha_{12}\rvert^2$
Incident field polarization	⟨100⟩	⟨100⟩	⟨110⟩	⟨110⟩
Scattered field polarization	⟨100⟩	⟨010⟩	⟨110⟩	⟨1$\bar{1}$0⟩

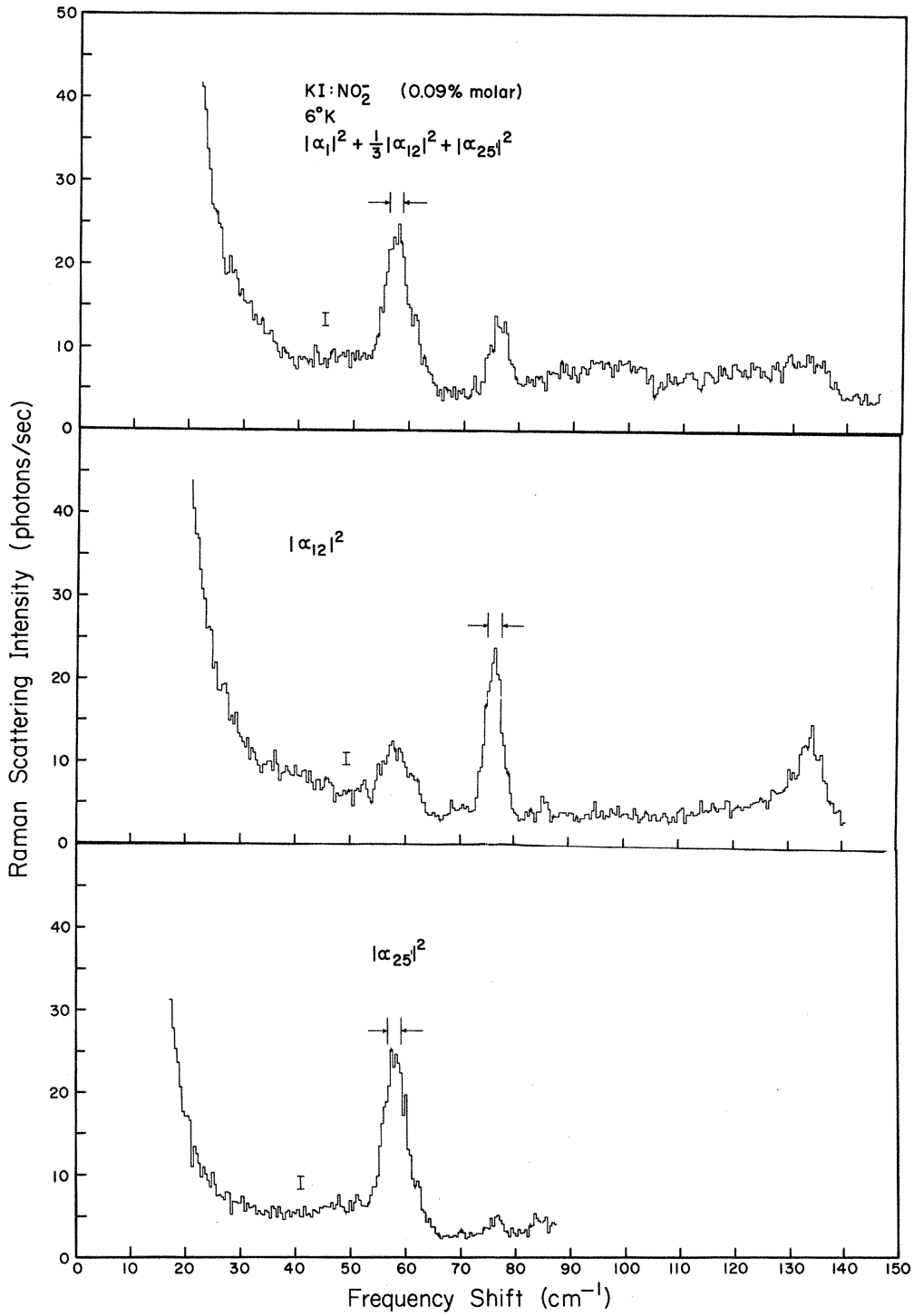

FIG. 4. Polarized Raman spectra for KI:NO_2^- at 6 °K. Spectra were measured for the polarizations and orientations listed in Table II.

of the laser. Intensities were measured in photon counts for a fixed time constant and slit width and were corrected for the frequency-dependent response of the spectrometer. The relative intensities are listed in Table III.

At 80 °K, the peaks in KI are still visible against

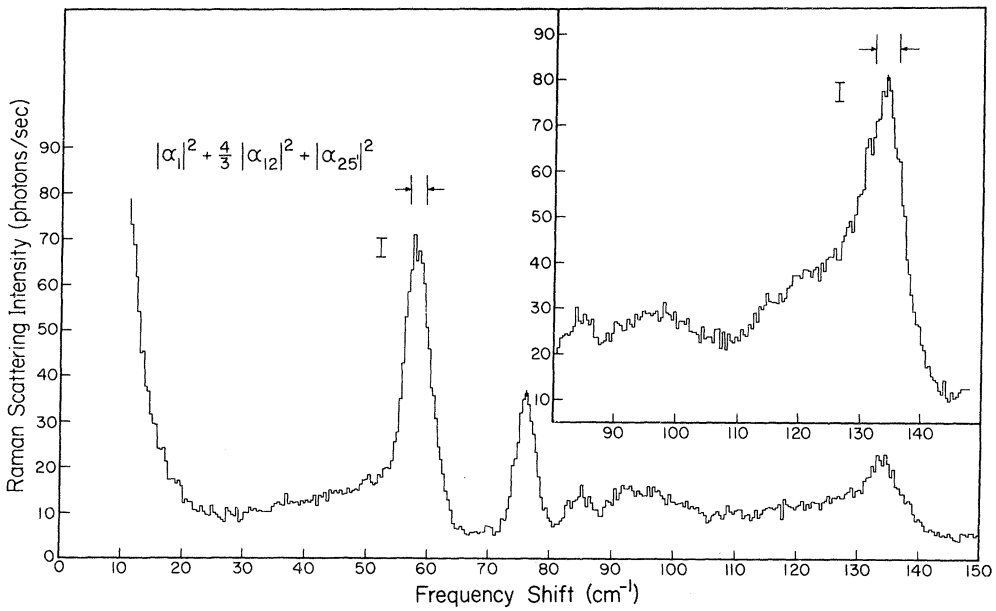

FIG. 5. Unpolarized Raman spectrum of KI:NO_2^- (0.09% molar) at 6 °K. Inset shows part of the spectrum at higher sensitivity.

the stronger two-phonon background. The 75-cm^{-1} gap mode is now at ~ 72 cm^{-1}, with approximately the same width and strength.

B. Vibronic Spectra

Each of the nitrite-doped crystals showed a broad absorption band in the near uv. At liquid-helium temperature this band developed a rich variety of structure, as shown in Fig. 6 for KCl : NO_2^-. The band consists of a series of prominent vibronic lines, each of which is accompanied by "phonon" sidebands. Each vibronic line also displays some rotational fine structure under higher resolution.

The rotational fine structure and phonon sidebands are shown for the first (0, 0) or second (0, 1) vibronic line in each crystal in Fig. 7. For higher vibronic lines there is some overlap of phonon sidebands and the rotational structure differs somewhat, as shown at higher resolution in Fig. 8.

TABLE III. Dependence of Raman intensity on frequency of exciting light for 76-cm^{-1} gap mode in KI:NO_2^- at 6 °K.

Laser wavelength (Å)	Predicted relative intensity	Measured relative intensity (±10%)
5145	1.0	1.0
4880	1.7	1.6
4579	3.3	3.0

These spectra also were measured at temperatures below 4.2 °K. For instance, the rotational structure of the pure electronic (0, 0) vibronic line in KCl is shown at 1.5 and 4.2 °K in Fig. 9. Qualitatively similar temperature effects occur in the fine structure of the other vibronic lines in KCl.

Measurements of the effects of uniaxial stress were also made. In KCl : NO_2^- the most pronounced effect is a stress-induced dichroism throughout the whole absorption band caused by alignment of the molecule under [110] stress. For the KCl sample with a [110] stress of ~5 kg/mm^2 at 2.1 °K, the absorption of light polarized parallel to the stress increases by a factor of 2.5, whereas that polarized in the [1$\bar{1}$0] direction decreases by about half. A stress of 8 kg/mm^2 causes the [1$\bar{1}$0] component of absorption to vanish into the noise. For the KBr sample a [110] stress of 5 kg/mm^2 causes the absorption of light polarized parallel to the stress to increase by a factor of 2.5, while that polarized in the [1$\bar{1}$0] direction decreases by at least a factor of 8, where it is buried in the noise. The effect of [110] stress on the rotational fine structure components in KCl and KBr is shown in Fig. 10. For [100] stresses up to 5 kg/mm^2, no splitting or shifting of the line components was observed.

Clarke has made a very preliminary measurement of the effect of hydrostatic pressure[8] on KCl: NO_2^- at 4.2 °K, using an optical pressure cell with helium as the pressure medium.[9] The only

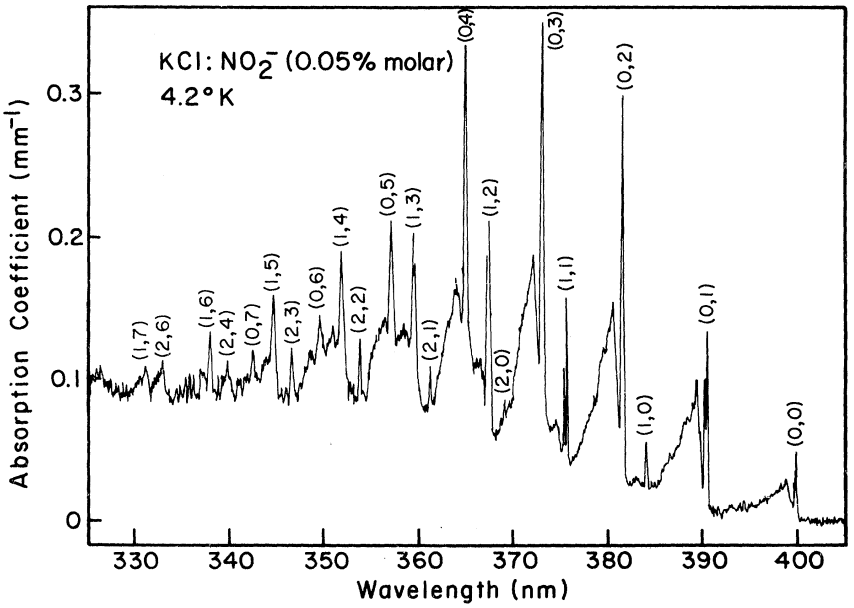

Fig. 6. Vibronic absorption band of KCl:NO_2^-. The vibronic lines $\nu^{abs}_{n_1 n_2}$ are designated by the quantum numbers n_1 and n_2, corresponding to the number of modified stretching- and bending-mode quanta excited.

change appears to be a uniform shift of the vibronic structure to higher energy by ~ 25 cm^{-1} at ~ 5 kbars (~ 50 kg/mm^2).

The KBr : NO_2^- samples sometimes show an anisotropy of as much as a factor of 2 in the vibronic absorption of polarized light before the application of stress. This anisotropy is observed in unstressed samples at 4.2 °K, but occasionally it increases somewhat after stress has been applied at lower temperatures. It is apparently due to internal strain in the crystal, which has caused a preferential orientation of the NO_2^- molecules.

In KI : NO_2^- at 2.1 °K, a [110] stress of 3 kg/mm^2 causes the pure electronic (0, 0) vibronic line, which has no resolved fine structure at zero stress, to split in parallel polarization by about 10 cm^{-1}, with one component remaining at a fixed position and the other component increasing in energy. Higher stresses cause the shifted component to grow in intensity while the unshifted component decreases, until at 6 kg/mm^2 – the maximum stress attained – it is three times as large as the unshifted component. At the same time, in $[1\bar{1}0]$ polarization the absorption line broadens, with a shoulder appearing on the low-energy side. This shoulder is never resolved but appears to correspond to a shift of the line by an amount opposite and about equal to that observed in parallel polarization. Stress splitting of the (0, 0) line is shown in Fig. 10. The effect of the [110] stress on higher vibronic lines is similar. With [100] stress up to 5 kg/mm^2, no broadening or shifting of the lines is observed. The anisotropy at zero stress sometimes observed in the KBr : NO_2^- samples can also be seen in the KI : NO_2^- samples.

IV. INTERPRETATION OF NITRITE-INDUCED SPECTRA

A. Internal Structure of Nitrite Ion

The nitrite ion is a bent O – N – O molecule of C_{2v} symmetry.[10] Its normal modes are shown in Fig. 11. They are the symmetric stretching mode $\nu_1(A_1)$, the symmetric bending mode $\nu_2(A_1)$, and the asymmetric stretching mode $\nu_3(B_1)$. It is known from x-ray crystallographic studies[11] and infrared measurements[1] that the N – O bond length is 1.24 Å and the O – N – O bond angle is 118° when the molecule is in its ground state. The frequencies of these modes are listed in Table IV for the alkali-halide hosts studied in this work. It is clear that the internal vibrations are only slightly perturbed by the host lattice.

The lowest-energy electronic transition of the nitrite ion gives rise to the vibronic absorption band in the near uv. This has been assigned to a $^1A_1 \rightarrow {}^1B_2$ transition ($n_N \rightarrow \pi_3$ in the notation of Ref. 12), in which one of the unshared electrons on the nitrogen atom is promoted to an antibonding π orbital of the ion. This involves a redistribution of electronic charge from the nitrogen atom to the two N – O bonds, and its principal effects are an increase in the bond angle and an alteration of the normal-mode frequencies in the excited state. The transition dipole moment is known to be perpendicular to the plane of the molecule.

The change in equilibrium configuration between the ground and excited states is reflected in the vibronic spectrum for KCl : NO_2^- in Fig. 6. The pure electronic transition at 400 nm is accompanied by a long series of vibrational sidebands.

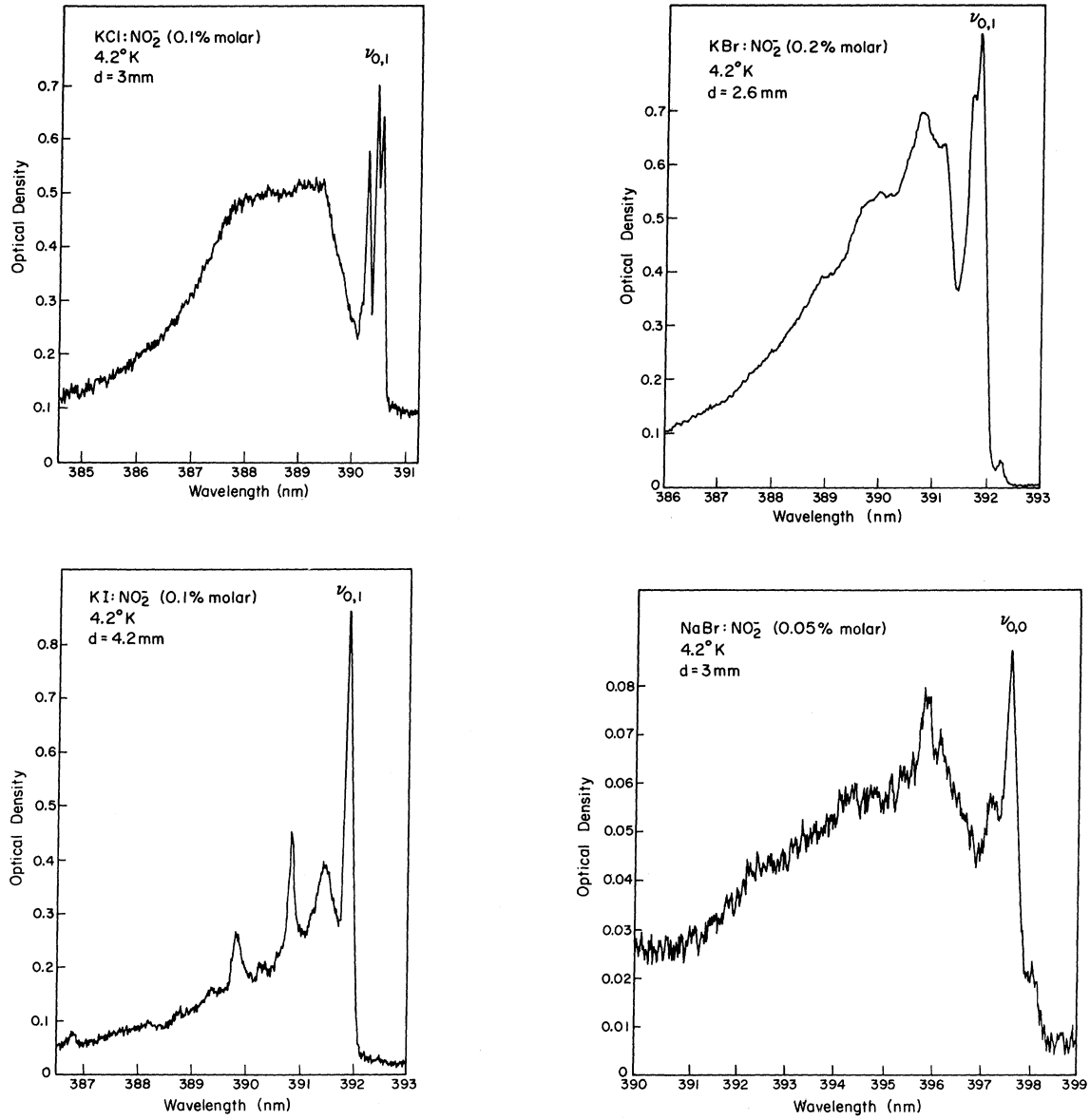

FIG. 7. Sideband structure associated with particular vibronic lines in the uv absorption of NO_2^- in four different hosts.

Their positions are given by the formula

$$\nu^{abs}_{n_1,n_2} = \nu_{0,0} + n_1\nu_1' + n_2\nu_2' , \quad (1)$$

where $\nu_{0,0}$ is the frequency of the pure electronic transition, ν_1' and ν_1' are the excited-state stretching and bending mode frequencies, respectively, and n_1 and n_2 are non-negative integers. In the figure it is possible to distinguish peaks corresponding to $n_1 = 0$, 1 or 2 and $n_2 = 0$, 1, ..., or 7. The strongest transition is $\nu^{abs}_{0,3}$.

Using a Franck-Condon analysis of the relative intensities of the NO_2^- vibronic lines, Sidman[12] inferred that the O – N – O bond angle changes (presumably increases) by $9° \pm 4°$ in the excited state, while the bond length changes only slightly, if at all.

The corresponding $^1B_2 \rightarrow {}^1A_1$ emission band has been observed in KCl and KBr by Timusk and Staude[4] and in KCl, KBr, and KI by Avarmaa[13] and Avarmaa and Rebane.[14] The intensity in emission is very weak and was not seen in the present work. A formula similar to that for absorption gives the positions of the vibronic emission lines

$$\nu^{em}_{n_1,n_2} = \nu_{0,0} - n_1\nu_1 - n_2\nu_2 . \quad (2)$$

Here ν_1 and ν_2 are now the ground-state stretching

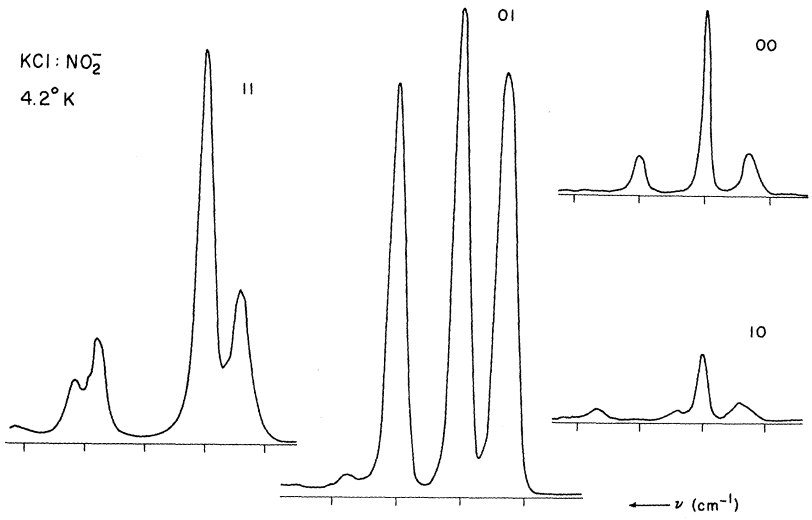

FIG. 8. Microdensitometer tracing of rotational structure of several vibronic absorption lines for KCl: NO_2^- at 4.2 °K. Scale marks indicate 10-cm^{-1} intervals with respect to central peak.

and bending frequencies, and n_1 and n_2 have the same meaning as in (1). These frequencies are listed in Table IV, and agree with the infrared results.

The ground-state modes also appear in our Raman spectra (Figs. 1 and 2). The low-temperature frequencies are listed in Table IV, and are seen to be in good agreement with those determined from other spectra. The relative intensities of the lines are in good agreement with Raman spectra for the NO_2^- in aqueous solution and in crystalline $NaNO_2$.

B. Interaction of Nitrite Ion with Host Lattice

Section IV A described those features of the nitrite spectra which are quite insensitive to the host lattice. Now we turn to those that depend critically on the particular host lattice.

In this section we consider how the nitrite ion oscillates and rotates as a rigid body in the anisotropic potential of the halogen vacancy. For some purposes we will assume that this is a rigid potential. For others, we will assume that it is modulated by the vibrations of the surrounding lattice ions. In either case, the potential will depend on the electronic state of the molecule and perhaps also on its vibrational state.

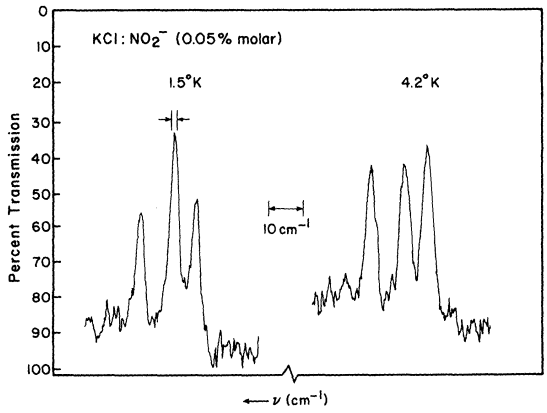

FIG. 9. Temperature dependence of rotational structure on the (0,0) line of KCl:NO_2^-.

The location and orientation of the molecule in the cavity may also affect the potential which determines its motion. At high temperatures the molecule probably rotates or tumbles in the cavity nearly freely, with the surrounding ions adjusting adiabatically to the changes in orientation. However, at sufficiently low temperatures the molecule tends to have certain preferred orientations.

1. *Orientation*

From the evidence presented here and elsewhere, we will show that the correct orientation is that of Fig. 12, in which the symmetry axis of the NO_2^- molecule lies in a [110] direction and the molecular plane is a (110) plane. Because there is the most evidence for KCl, we begin the discussion there. First, the [110] orientation of the molecular symmetry axis was established by Narayanamurti, Seward, and Pohl (NSP)[1] on the basis of stress-induced dichroism in the infrared absorption. They found that all the molecules could be aligned in the $[1\bar{1}0]$ direction using a [110] uniaxial stress of ~ 5 kg/mm^2 at 2 °K. They also concluded from observations of the ν_3 absorption line that the plane of the molecule is a (110) plane, although the dichroism for ν_3 is much smaller, so that the evidence in this case is somewhat weaker. However, the (110) orientation for the plane of the molecule is demonstrated conclusively by our stress-induced

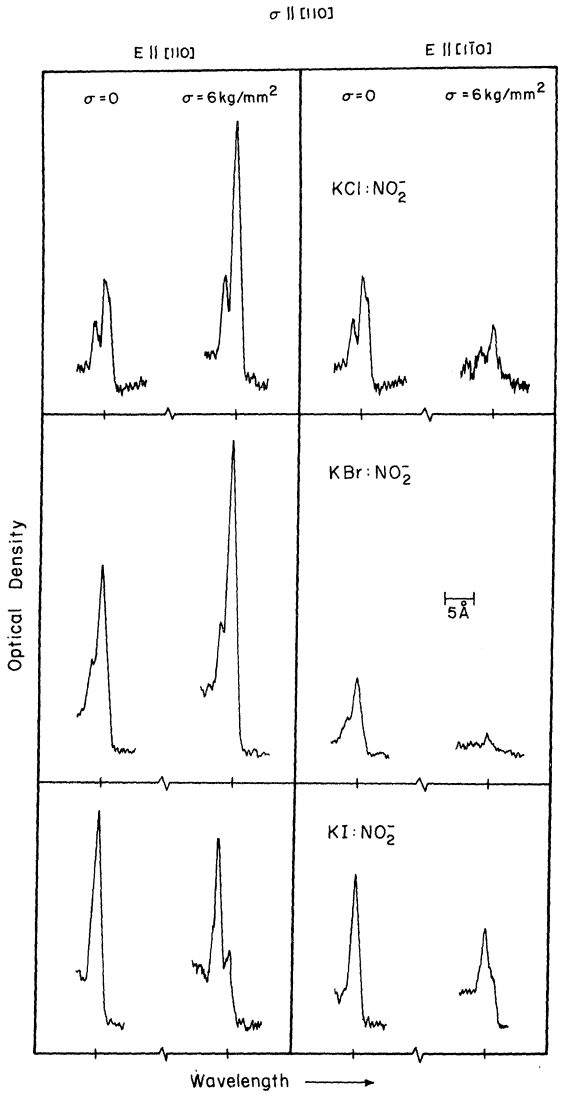

FIG. 10. Effect of [110] stress on the $\nu_{0,0}$ absorption line of the nitrite ion in KCl, KBr, and KI at 2 °K. Spectra for light polarized parallel and perpendicular to the stress direction are shown with and without applied stress. The scale marks indicate in each case the position of the main peak for zero stress.

dichroism in the uv absorption. When all the molecules are aligned along [1$\bar{1}$0] they must lie in (110) or (100) planes, since the molecule is not rotating about its symmetry axis at 2 °K in KCl.[1] The uv-transition dipole moment is perpendicular to the plane of the molecule, so the stress-induced increase in [110] absorption for a [110] stress implies that the normal to the plane is in the [110] direction. Finally, the nearly on-center position for the NO_2^- ion in the cavity follows from measurements of the dielectric relaxation by Sack and Moriarty.[15] They found that the contribution from molecular reorientation to the dielectric response of the crystal persisted to the lowest temperatures, and that it implied a dipole moment of 0.21 D as expected for the dipole moment of the molecule at the center of the cavity. From the similarity of the stress-induced dichroism of the vibronic spectra, we assume that the orientation in KBr is the same as that in KCl and that the molecule is able to reorient under stress.

However, in KI : NO_2^- Sack and Moriarty found a much larger dipole moment (1 D) and an activation energy of 0.014 eV (115 cm^{-1}) for reorientation. Although their interpretation is less definite in this case, both these results imply that the NO_2^- takes an off-center position in the cavity. Because of the high polarizability of the I^- ions which would tend to attract the positive nitrogen atom, one might suspect that the symmetry axis of the NO_2^- would point in a ⟨110⟩ direction.

The uniaxial stress measurements for KI confirm this orientation. As shown in Fig. 10, a [110] stress causes the pure electronic (0, 0) vibronic lines (as well as higher vibronic lines) to split, but causes no dichroism. This can be understood if we assume that the stress removes the degeneracy of the various possible orientations of the type shown in Fig. 12, i.e., with the molecule symmetry axis along ⟨110⟩ and the O – O axis along ⟨001⟩. For a [110] stress, there will then be three inequivalent orientations as listed in Table V. The contribution of each to the absorption of light polarized parallel and perpendicular to the stress axis is also listed. If no reorientation occurs under stress, then the polarized spectra will resemble those shown in Fig. 10.

The system NaBr : NO_2^- has not been studied in the infrared, and its stress-induced dichroism has not been measured. From the similarity of its Raman spectra to those of the others studied, however, the same orientation seems probable. Therefore, we will assume that the NO_2^- ion is oriented

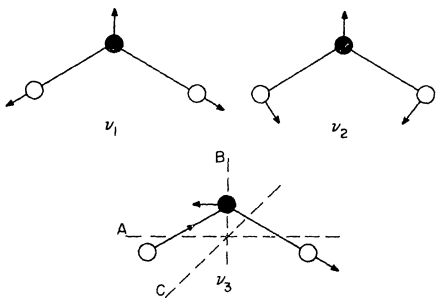

FIG. 11. Normal modes and rotation axes of the nitrite ion.

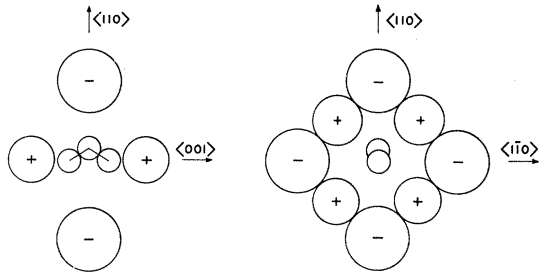

FIG. 12. Probable equilibrium orientation of the nitrite ion at low tempeatures in alkali halides. In some hosts, such as KI, the ion may be in an off-center position displaced towards the halide ion nearest the nitrogen atom.

the same in NaBr as in KCl.

2. *Vibrational Motion*

There has been much speculation about how the nitrite ion moves in this cavity. Spectral features in the range of lattice vibration frequencies have been observed in far-infrared spectra and as sidebands on uv and infrared transitions. These have been attributed variously to translational modes of the NO_2^- ion in its cavity, high-frequency librational modes, or perturbed lattice modes of the host. Some of these alternatives are supported and others ruled out by the Raman data presented here.

Raman spectra. Although much of the interpretation in this section is based on a formal theory of Raman scattering, it is useful to begin the discussion with the simple semiclassical theory, which will demonstrate the qualitative aspects of the Raman spectra. According to the theory of off-resonance Raman scattering,[16] the Raman intensity is approximately proportional to the quantity $\omega_0^4/(\omega_A-\omega_0)^2$, where ω_0 is the frequency of the laser light and ω_A is the frequency of the absorption contributing to the polarizability responsible for the Raman scattering. For the case of the nitrite ion in an alkali halide and laser excitation at 4880 Å, the most important contribution to the polarizability comes from the uv transitions of the NO_2^- ion, which are reflected in the vibronic absorption spectrum. If for the moment we replace this broad detailed absorption band by a single band at $\omega_A \sim 3700$ Å, the most intense region of the spectrum, then the predicted relative intensities of the Raman spectra agree reasonably well with the measured values, as shown in Table III for the 76-cm^{-1} gap mode in $KI:NO_2^-$, indicating that the Raman scattering is, in fact, primarily dependent on the polarizability of the nitrite.

We are primarily concerned about how this polarizability, expressed in the fixed frame of the crystal, is modulated during various motions of the NO_2^- ion and its neighbors. For some types of motion the polarizability varies linearly with displacement, and for others it varies quadratically. For a motion in the crystal at frequency Ω, the former case will give rise to first-order Raman scattering at $\omega_0 \pm \Omega$, the latter to second-order scattering at $\omega_0 \pm 2\Omega$. For example, translational oscillation of a monatomic impurity is an odd-parity mode and will not give rise to first-order Raman scattering. For the NO_2^- impurity, we assume that, in first approximation, parity is still a good quantum number because the NO_2^- ion is much smaller than the cavity in which it moves and therefore distorts the cubic symmetry of the cavity very little. The translational oscillation at the center of inversion will again not be Raman active in first order, although oscillation at a site which is not a center of inversion will be Raman active as will modulation of the polarizability by even-parity vibrations of the surrounding ions, such as those shown in Fig. 13. Libration of the molecule about its equilibrium position may or may not be Raman active in first order, depending

TABLE IV. Internal vibrational frequencies of NO_2^- in alkali halides.

		Infrared (Ref. 1) ($T=2$ °K) (cm^{-1})	Vibronic emission (Refs. 13, 14) ($T=4.2$ °K) (cm^{-1})	Raman (this work) ($T=6$ °K) (cm^{-1})	Vibronic absorption (Ref. 14, this work) ($T=4.2$ °K) (cm^{-1})
KCl	ν_1	1327	1313	1327	1024
	ν_2	803	800	806	599
	ν_3	1290	···	1286	···
KBr	ν_1	1318	1310	1317	1011
	ν_2	798	795	800	595
	ν_3	1276	···	1274	···
KI	ν_1	1308		1305 1314	997
	ν_2	805	805	806	604
	ν_3	1253	···		···
NaBr	ν_1			1327	1020
	ν_2			828	636
	ν_3		···	~1283	···

TABLE V. Contributions to stress shift in $KI:NO_2^-$.

		$\sigma \parallel [110]$			
Orientation	Number	$I_{\parallel}$	:	I_+	Shift
(110)	2	1		0	+
(011)	8	$\frac{1}{4}$		$\frac{1}{4}$	0
(1$\bar{1}$0)	2	0		1	−

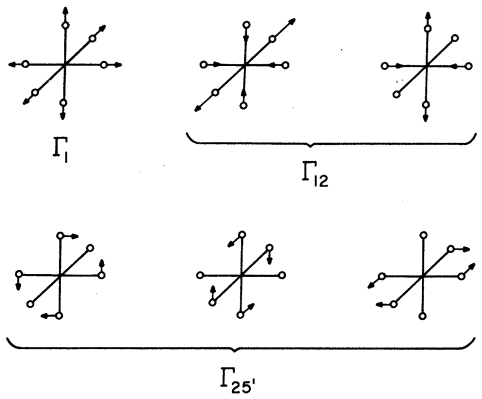

FIG. 13. Even-parity vibrations of the nearest-neighbor ions at a site of O_h symmetry.

on the relative orientation of the electric field and the molecule. Consideration of the polarizability ellipsoid, which is a general ellipsoid with one axis parallel to the symmetry axis of the ellipsoid of the molecule, shows that if the electric vector is parallel to an axis of the ellipsoid of the molecule in equilibrium position, no first-order Raman scattering is allowed. Therefore, it can easily be seen that, for example, in the case of a [100] incident electric field, four of the "equivalent" ⟨110⟩ orientations of the molecule will not have first-order Raman-active librations about their equilibrium orientations, whereas the remaining eight will. These same considerations can be applied to rotations, which will be discussed in more detail later.

The polarization of the Raman scattering gives additional information about the components of the polarizability which are being modulated, and therefore about the symmetry types of motions, as listed in Table II.

KI: We start with the nitrite-induced spectra in KI because these show the best resolved structure. The most prominent features are the peaks at 58, 76, and 133 cm^{-1} shown in Fig. 4. From these polarized spectra, it is seen that the 58-cm^{-1} peak corresponds to a mode which is primarily $\Gamma_{25'}$, the 76-cm^{-1} peak is almost entirely Γ_{12}, and the 133-cm^{-1} peak is mostly Γ_{12}. In addition to these sharp features, it should be noted that there are other weaker features at ~95 and ~115 cm^{-1}, as shown most clearly in Fig. 5. The sharp peak at 76 cm^{-1} lies in the gap between acoustic- and optic-phonon frequencies (69.7–95.6 cm^{-1}).[17]

The positions of these peaks are compared in Table VI with the positions measured for peaks in the far-infrared spectra[8,18,19] and in near-infrared[1] and vibronic sidebands.[4,13,14] The Raman lines are nearly all at different positions. In preliminary measurements,[7] it appeared that the Raman line at 76 cm^{-1} and the far-infrared line at ~79 cm^{-1} were the same, but we have repeated the Raman measurement with greater care to determine the position given in the table, 76 ± 1 cm^{-1}.

Recently, Hughes[6] has repeated the far-infrared measurement with higher resolution on one of our KI: NO_2^- samples. He saw two sharp lines (half-width less than 0.5 cm^{-1}) at 71 and 80 cm^{-1}, broad weak bands at 55 and 63 cm^{-1}, and virtually no absorption below 40 cm^{-1}. Thus we are quite confident that the differences are not sample or concentration-dependent effects.

The differences imply that the peaks at 71 and 80 cm^{-1} may correspond to motions which are not Raman active in first order. These modes may be translational modes of the impurity about a center of symmetry. Sharp "gap modes" in this frequency range are a common feature of far-infrared impurity spectra in KI, and are observed for monatomic impurities as well as molecules. Translational modes of the molecule parallel to its A, B, and C axes are possible. These would all be infrared active, but only the second could be Raman active in first order. It is possible that the differences in peak position seen in the Raman and far-infrared spectra may correspond to different rotational excitations accompanying the

TABLE VI. "Lattice" vibrational structure in KI:NO_2^-.

Investigator	Ref.	Technique	Energy (cm^{-1})								
Renk	18	Far infrared			65		71		79		
Sievers and Lytle	19	Far infrared		55	63.5		71.2		79.5		
Hughes	8	Far infrared		55	63		71		80		
NSP	1	Near infrared		53	63		71		79	137	206
									80.5		
This work		Raman		58				76		133	
Timusk and Staude	4	uv abs.	21.4		63.5		70			136	206
Avarmaa	13	uv abs.	...			66				133	200
Avarmaa and Rebane	14	uv abs.	17			...				...	...
This work		uv abs.	26			69				134	

same translational mode, but such an interpretation does not appear probable.

If the NO_2^- ion in KI were quite well localized in an off-center position (lacking inversion symmetry) and if it oscillated about that equilibrium position, then this oscillation would be both Raman and infrared active. However, such an oscillation, when averaged over equivalent orientations of the molecule, would be seen with approximately equal intensity in the $|\alpha_1|^2$, $|\alpha_{12}|^2$, and $|\alpha_{25'}|^2$ spectra, even if some nonrandom orientation of the NO_2^- is allowed. No such mode is seen in the Raman spectra measured, so we conclude that the parity selection rule still applies.

NSP[1] have suggested that the infrared lines correspond to high-frequency librational modes of the molecule about its c.m. Although such an interpretation is possible in terms of the simple considerations stated above, it is probably incorrect. Both such modes would be Raman active in a crystal containing NO_2^- ions randomly oriented in the $\langle 110 \rangle$ equilibrium positions, but two such modes are not seen in the Raman spectra. Furthermore, the similarity of the KI spectrum to those discussed below for other hosts suggests that the Raman-active modes in KI:NO_2^- are not strongly dependent on the off-center position of the NO_2^- ion in KI, as required for the interpretation in terms of librational modes.

We propose that the Raman peaks correspond to a different class of motions, the perturbed vibrations of neighboring lattice ions. If we assume that only the motions of the nearest-neighbor ions will have a significant effect on the polarizability, then the important modes for a site of O_h symmetry are those shown in Fig. 13. Only those modes of even parity Γ_1, Γ_{12}, and $\Gamma_{25'}$, are Raman active, and their polarization selection rules are listed in Table II.

A procedure for predicting the impurity-induced Raman spectra due to perturbed lattice modes has been presented by Benedek and Nardelli[20] for the case of the F center in alkali halides. It is based on the formal theory of off-resonance impurity-induced Raman scattering due to Maradudin.[21] The perturbations to the lattice dynamics are assumed to be the change in mass at the impurity site and a change in nearest-neighbor force constants for the impurity. If the unperturbed phonon eigenvectors are known, then the perturbed eigenvectors and frequencies can be calculated by Green's-function techniques. It should be pointed out, though, that this calculation is not entirely appropriate for the case of NO_2^-. It assumes that the defect is spherically symmetric and on-center at a site of O_h symmetry, and that only nearest-neighbor interactions are important.

For the case of Stokes scattering, this model predicts that the defect-induced first-order Raman spectrum has spectral density $S_\Gamma(\Omega)$, where

$$S_\Gamma(\Omega) \propto \{[N(\Omega)+1]/\Omega\}\rho_\Gamma(\Omega) \qquad (3)$$

for symmetries Γ_1, Γ_{12}, and $\Gamma_{25'}$. Here $\rho_\Gamma(\Omega)$ is the perturbed-crystal projected density of states for phonons of symmetry type Γ, and $N(\Omega) = [\exp(-\hbar\Omega/k_B T) - 1]^{-1}$. Page[22] has computed projected densities of states for these symmetries for a range of fractional changes in force constant $\Delta k/k$. For his phonon frequencies and eigenvectors, he used the breathing-shell-model results,[23] which are in good agreement with those of the Cowley shell model[24] based on recent inelastic neutron scattering data.[17]

The decreased force constant has a dramatic effect on the densities of states of KI. As the force constant is decreased from its unperturbed value, the intensity of the optic modes decreases, and the intensity of the acoustic modes increases. These changes occur more or less smoothly and monotonically with decreasing force constant. Only a slight reduction of the central force constant k_L is adequate to pull a part of the Γ_{12} optic branch into the phonon gap. As the force constant is lowered, this gap mode decreases in frequency. A Γ_1 gap mode also exists for central force-constant changes of 80% or greater. The projected densities of states for $\Delta k/k = 0$ and -0.8 are shown for KI in Fig. 14. The $\Gamma_{25'}$ density of states is not affected by a change of central force constant. Thus, the calculated curve for the unperturbed $\Gamma_{25'}$ density of states in Fig. 14 presumably also holds for nonzero Δk.

The best fit to the KI data for the different symmetry types seems to be for about $\Delta k/k = -0.8$. The feature which is most sensitive to this choice is the position of the 76-cm^{-1} gap mode, whose polarization indicates that it is almost purely Γ_{12} symmetry. In the curves showing the calculated densities of states, the predicted Γ_{12} gap mode is represented by a rectangle with a width of 2 cm^{-1}, comparable with the width of the observed gap mode, and an area which indicates its strength. Its integrated intensity was estimated from the normalization requirement for the Γ_{12} projected density of states to be approximately one-third that of the in-band (acoustic and optic) Γ_{12} modes.

The intensity scale of the Γ_{12} experimental spectrum is fitted to the height of this gap mode in Fig. 14. The Γ_1 and $\Gamma_{25'}$ experimental spectra are drawn to this same scale (i.e., we have not accounted for any difference in coupling to modes of these symmetries). The intense peaks below 40 cm^{-1} predicted by the model for all three symmetries were not seen in the Raman spectra, even

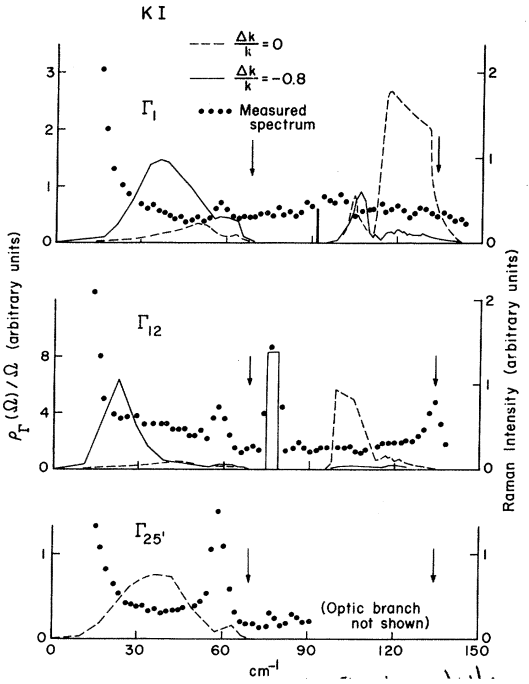

FIG. 14. Comparison of measured Raman spectra (cf. Fig. 4) with the calculated projected densities of states for KI. The strength of the 76-cm^{-1} gap mode in the perturbed Γ_{12} spectrum was used to determine the relative scales. The vertical arrows indicate the positions of peaks in the vibronic sidebands.

after a careful search with spectrometer slits sufficiently narrow to permit observation within 20 cm^{-1} of the Rayleigh peak and good photon statistics. In earlier work on KI crystals with the heaviest doping, some of the broad peaks showed different relative intensities, and an additional peak at 25 cm^{-1} was observed. Because this peak does not appear at lower concentrations, it must not be due to isolated NO_2^- ions.

The predominance of the Γ_{12} contribution to the Raman spectra can be understood qualitatively in terms of the stress behavior noted earlier for the vibronic line in KI. That is, following the approach of Benedek and Nardelli, [20] the coupling of the polarizability to phonons of different symmetries can be taken as proportional to the shift of the transition energy for static strains of the same symmetry.

In our case, the vibronic line showed a resolved splitting for [110] stress, but no effect for [100] stress, implying that the dominant coupling is to Γ_{12} (tetragonal) strain.

NaBr: Sodium bromide also has a gap in the phonon spectrum (105–126 cm^{-1})[25] and the nitrite-induced Raman spectra are qualitatively similar to those of KI. There is a prominent gap mode at 109 cm^{-1} which is almost entirely of Γ_{12} symmetry. We assume that the interpretation is similar to that of KI, although we have much less information for NaBr. The best fit for the projected densities of states is obtained for $\Delta k/k=-0.4$ (cf. Fig. 15). This choice is determined most sensitively by the position of the gap mode. Far-infrared spectra are not available for NaBr.

KBr: There is only a small phonon gap in potassium bromide (94–102 cm^{-1}).[24] Thus the prominent Raman peak at 88 cm^{-1} is a resonance mode just at the edge of the gap. It is again predominantly Γ_{12}. The spectra can be fitted approximately for $\Delta k/k=-1.0$, although this choice is much less well determined than for the preceding cases. We assume that the interpretation follows that of KI.

KCl: Potassium chloride has no phonon gap,[26] and the nitrite spectra show no sharp peaks in this case. The strongest feature is the broad peak at ~ 50 cm^{-1}, which is again of Γ_{12} symmetry. It can be fit quite well with $\Delta k/k=-0.7$.

Thus all the nitrite-induced Raman spectra seem to be consistent with the interpretation that perturbed lattice vibrations of Γ_{12} symmetry are the dominant feature. The nearest-neighbor force constants appear to be reduced [by 40% in sodium bromide and by (80 ± 20)% in the potassium halides] because of the smaller repulsive potential when the NO_2^- ion is present than when a halogen ion is present. It should be pointed out that the force-constant changes chosen for the potassium halides exceed those necessary in the breathing shell model to produce a Γ_{15} ("off-center") instability.[22]

Vibronic spectra. The sidebands on the vibronic "zero phonon" lines in the uv spectrum of NO_2^- also give information about the perturbed lattice modes. These modes are excited when the molecule makes the $^1A_1 \rightarrow {}^1B_2$ electronic transition because the equilibrium positions of the surrounding ions are altered. The electron-lattice coupling for local modes and phonons has been discussed by many authors.[21,27]

The sidebands for the emission lines $\nu^{em}_{n_1,n_2}$ correspond to the ground-state motions we have been discussing. These spectra have only recently been measured with the necessary resolution, in KCl and KBr, by Avarmaa.[13]

The sidebands in absorption apply to the motions for the $^1B_2$ excited state. In general, these will differ because of the change in molecular geometry and charge distribution, and the consequent changes in coupling to the surrounding lattice.

If the impurity is at a center of symmetry, then the lattice sidebands are caused by modes of the same symmetries as in Raman scattering, i.e., Γ_1, Γ_{12}, and $\Gamma_{25'}$. There probably will also be

some excitation of the longitudinal translational mode of the nitrite ion.

KCl: We start with KCl because both absorption and emission sidebands have been measured for it. These have only relatively broad features.

The sidebands on the emission lines have been measured at 4.2 °K by Avarmaa, who finds a series of three broad maxima at 75, 155, and 230 cm^{-1}, compared to similar maxima at 65 and 125 cm^{-1} in absorption. This result implies that the appropriate force constants are smaller in the excited state.

The broad background features of the sideband spectrum are consistent with Γ_1 and Γ_{12} projected densities of states for a force-constant reduction of ~ 70%, as estimated for the Raman results (cf. Fig. 15).

KBr: The absorption and emission sidebands have also been measured for KBr by Avarmaa and are quite similar to those of KCl, showing a very slight reduction in frequencies in the excited state. The peak positions in absorption are 43, 68, 135, and 195 cm^{-1}; those in emission are 70, 140, and 210 cm^{-1}. A rather less than striking fit to the absorption spectrum is obtained for $\Delta k/k = -1.0$, as seen from reference to Fig. 15. This fit does allow an interpretation of the 11-cm^{-1} peak, but this peak is believed to be correctly interpreted as part of the rotational fine structure to be discussed later. It would seem more reasonable to consider the 70-cm^{-1} peak in emission to be a longitudinal translational mode of the impurity, with the corresponding mode at 68 cm^{-1} in absorption. Then a series of three excitations of this mode is seen in each spectrum.

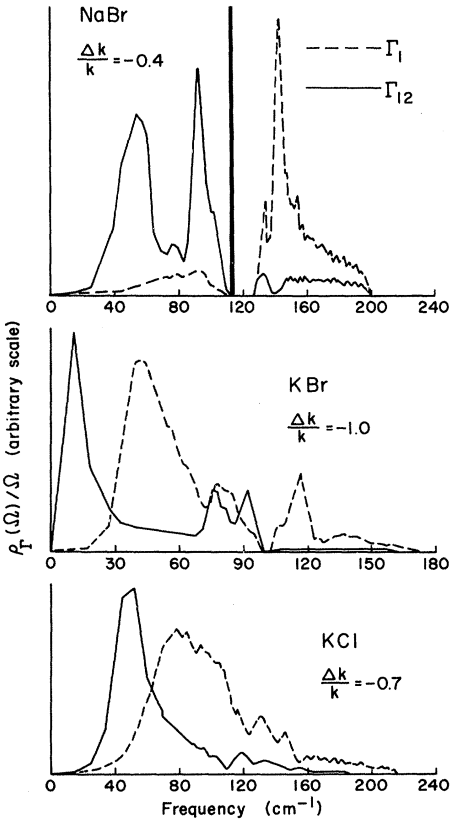

FIG. 15. Calculated projected densities of states for perturbed Γ_1 and Γ_{12} modes in KCl, KBr, and NaBr. The curves are drawn for the value of $\Delta k/k$ which gives the best apparent fit to the data in each case.

Timusk and Staude[4] identified some of these features with critical points of the unperturbed lattice phonons. This correlation would seem to be somewhat fortuitous.

KI: Apparently the emission sidebands for KI have not yet been measured. This is unfortunate, because much more is known about the NO_2^- modes in KI than in the other hosts. It would be particularly interesting to see whether the 76-cm^{-1} Raman peak or the 71- or 79-cm^{-1} infrared peaks appear in emission.

In absorption, the most prominent sideband features are a broad peak at ~ 20 cm^{-1}, a sharp peak at 69 cm^{-1}, a broad peak at 134 cm^{-1}, and a much weaker peak at ~ 206 cm^{-1}. These latter three might be a series corresponding to excitation of the translational impurity mode. Presumably this corresponds to the 79-cm^{-1} far-infrared mode, but with reduced force constants. It is suggested in the next section that the ~ 20-cm^{-1} band may be a librational mode. An alternative interpretation of all these features in terms of perturbed phonons is also possible (Fig. 14). In this interpretation the 69-cm^{-1} peak, which occurs at the edge of the phonon gap, would correspond to the gap mode discussed earlier, with force constants reduced in the electronic excited state. A comparison of crystals containing the normal $N^{14}(O^{16})^-_2$ ions with crystals containing isotopically enriched $N^{15}(O^{16})^-_2$ ions would be useful in interpreting the gap modes seen in the vibronic spectra. Modes which involve motion of the ion would show a change in frequency, while modes which involve only motions of the neighboring ions would not. It would also be interesting to use an isotopically enriched crystal to confirm the interpretation of the gap modes seen in the Raman and infrared work.

NaBr: The absorption sidebands of NaBr show peaks at 23, 62, 93, and 109 cm^{-1}. The line at 138 cm^{-1} reported by Timusk and Stuade was not found. The 109-cm^{-1} peak happens to be at the same position as the Raman "gap mode." The interpretation of the sidebands proposed here is

similar to that of KI and again offers the choice of explanation in terms of nitrite motion or perturbed phonons in the host. In the latter case, the 40% force-constant reduction fitted to the Raman spectrum is also reasonably appropriate for the vibronic spectrum.

3. *Rotational Motion*

The three principal rotational axes of the nitrite ion are shown in Fig. 11, and we label the corresponding moments of inertia I_A, I_B, and I_C, and the rotational constants $\tilde{A}$, $\tilde{B}$, and $\tilde{C}$ (where $\tilde{A} = h/8\pi^2 c I_A$, with h representing Planck's constant and c representing velocity of light). For the ground state of the molecule these are $\tilde{A} = 4.22$ cm^{-1}, $\tilde{B} = 0.45$ cm^{-1}, and $\tilde{C} = 0.43$ cm^{-1}. For the excited state, they should be $\tilde{A}' = 5.62$, $\tilde{B}' = 0.41$, and $\tilde{C}' = 0.39$, assuming that the bond angle increases by 9°.

The rotational motion of the nitrite ion in the ground-state configuration has been analyzed in detail by NSP[1] on the basis of the well-resolved fine structure on the infrared vibrational transitions.

Rovibronic structure. Somewhat similar fine structure is observed in our uv vibronic absorption spectra for certain hosts (Figs. 7 and 8). These spectra agree with the high-resolution absorption spectra recently reported by Avarmaa and Rebone.[14] The principal reason for the differences between these spectra and the infrared fine structure is that for the infrared transition the rotational constants and potential barriers remain nearly constant, whereas for the uv electronic transition they change appreciably. Any analysis must make allowances for these changes.

The model used by NSR to explain the infrared data is that of Pauling.[28] It assumes that a molecule is free to rotate about only one of its axes, that a twofold rotation about this axis takes the molecule into an identical configuration, and that the barrier to rotation about this axis is given by

$$V = \tfrac{1}{2} V_0(1 - \cos 2\theta) . \tag{4}$$

The Schrödinger equation for this potential is known as Mathieu's equation and its eigenvalues have been tabulated.[29] As a function of increasing V_0, the energy levels go over from those of a free one-dimensional rotor to those of a librator in a harmonic potential. Using this model, NSP were able to interpret their results primarily in terms of hindered rotation or libration about the A axis.

Avarmaa and Rebane[14] pointed out that, if the A axis lies in a ⟨001⟩ direction in the crystal, the hindering potential has four equivalent ⟨110⟩ orientations for the B axis, rather than two. Thus, the conclusions of NSP require modification, even if qualitatively correct.

Avarmaa and Rebane found reasonable agreement for both infrared and uv fine structure for the simplest assumption, a one-dimensional free rotor, provided they chose different rotational constants for the ground and excited states.

Earlier, Sauer[30] attempted to extend a more exact treatment to this problem, using the Devonshire model of a rigid rotor subjected to a potential field of octahedral symmetry. Choosing parameters consistent with the crystal field for NO_2^- in KCl with the orientation of Fig. 12, he solved numerically for the low-lying energy levels. However, he was unable to obtain good agreement between the infrared results and his predicted transition energies.

We choose to follow the original approach of NSP, except that we use a more appropriate hindering potential,

$$V = \tfrac{1}{2} V_0(1 - \cos 4\theta) . \tag{5}$$

The eigenvalues for this potential were determined using the method outlined by Koehler and Dennison.[31] This potential will affect the energy levels of the one-dimensional rotor as shown in Fig. 16. The levels for the free rotor are shown on the left ($E = \tilde{A}K^2$ for $K = 0, 1, 2, \ldots$), while those on the right are for the harmonic librator. The selec-

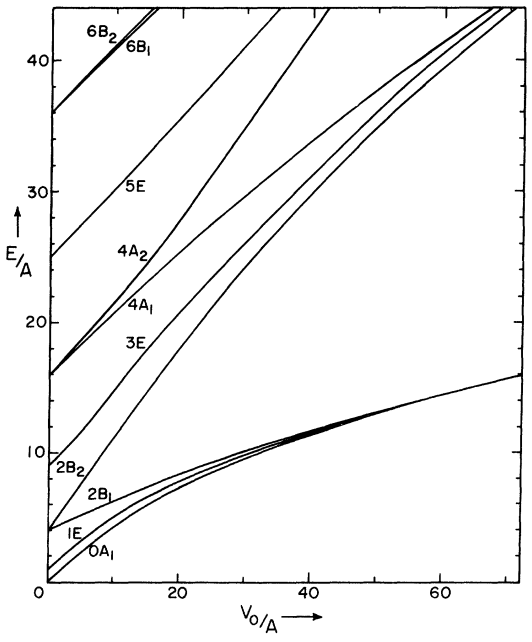

FIG. 16. Energy levels of the one-dimensional rotor of rotational constant A moving in the hindering potential $V(\theta) = \frac{1}{2}V(1 - \cos 4\theta)$.

tion rule is $\Delta K = \pm 1$; $\Delta k = \pm 3$ is also weakly allowed.

Using this simple model and the spirit of NSP's results, we are able to get quite good agreement with both the infrared and uv rotational fine structure.

KCl: NSP suggested that at low temperatures in KCl the NO_2^- ion undergoes hindered rotation about its A axis, and only small librations about its B and C axes. The ground-state levels which they deduced from the infrared structure are shown in Fig. 17. If we assume as they did that the nitrite rotates abouts its c.m., then the closest fit is obtained for $V/\tilde{A} \simeq 10$. The predicted energy levels for this choice are shown in Fig. 17. The agreement is not good, particularly for the level $2B_2$.

Avarmaa and Rebane proposed the alternative explanation that the nitrite rotates about an axis through the oxygen atoms when in the ground state. This seems reasonable if the oxygens are strongly bound to the potassium neighbors as implied in Fig. 12. In this case it would have $\tilde{A} \sim 2$ cm^{-1} instead of 4.22 cm^{-1}. For this choice, the ground-state energy levels are very nearly those of a free rotor ($V \sim 0$). The predicted levels for this choice are also shown in Fig. 17. We are inclined to favor this latter interpretation, although the evidence is not yet decisive.

For the vibronic spectra, the transitions occur

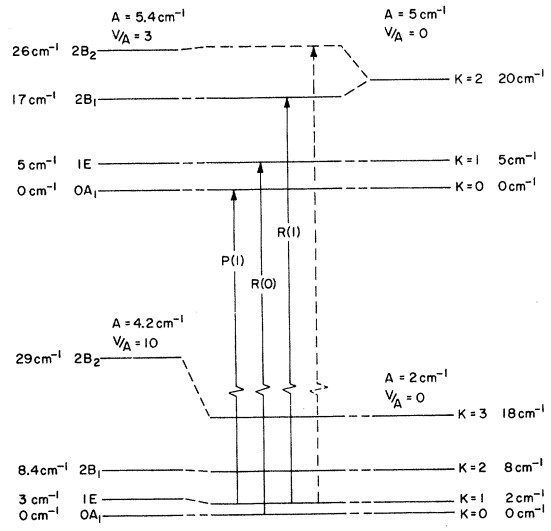

FIG. 17. Energy-level diagram for NO_2^- in KCl. The center section shows the energy levels and uv transitions inferred from the infrared and uv data. On either side are shown the corresponding levels for the hindered rotor (cf. Fig. 16), for particular choices of A and V. The dashed vertical line corresponds to the weak transition in the (0,1) rovibronic spectrum.

to rotational levels of the excited molecule. Avarmaa and Rebane suggested that these are nearly free rotor levels for $\tilde{A} = 5.46$ cm^{-1}, i.e., for the rotation axis through the center of mass. Figure 17 shows the excited state levels for $V = 0$ and $V = 3A$.

The temperature dependence of the major triplet shown in Fig. 9 confirms that the outer components originate from the $K = 1$ level in the ground state. In some of the high-resolution traces, the lines originating from $K = 1$ were split by 1–2 cm^{-1}. This is most likely from internal strain splitting of this twofold degenerate level.

The recent measurement of the rotational fine structure in emission at 4.2 °K by Avarmaa and Rebane also supports this assignment. They observed two lines separated by 6 or 7 cm^{-1}, in agreement with the emission spectrum predicted for this level diagram.

The rotational fine structure for higher vibronic transitions has somewhat different spacings and intensities. At least some of this difference can be understood qualitatively as a small dependence of the rotational constants on vibrational quantum number. A different explanation has been proposed for the more pronounced difference for the (1, n_2) vibronic lines.[14] This is the possibility of a Coriolis vibration-rotation interaction for the $K = 2$ level. Further experiments with temperature and stress at resolution comparable to that in Fig. 8 will be needed to assign all the rotational structure unambiguously.

KBr: Both the infrared[1] and vibronic[14] structure in KBr are qualitatively similar to those in KCl. Our stress-induced dichroism indicates that the nitrite ion is free to reorient, while the dielectric relaxation behavior found by Sack and Moriarty[15] shows that it does not reorient as easily as in KCl. Hence, we prefer not to assume free rotor levels, as Avarmaa and Rebane did, but suggest the choice $\tilde{A} \sim 2$ cm^{-1}, $V_0/\tilde{A} \sim 12$ for the ground state. Since there is a tendency for the nitrite to take an off-center position, this might appear as a small (e.g., ~ 2 cm^{-1}) splitting of the $K = 1$ level. This choice gives reasonable agreement with the observed transitions, but is quite arbitrary.

For the excited state levels seen in the vibronic spectra, the best fit is almost the same as for KCl, namely, a nearly free rotor with $\tilde{A} \sim 5$ cm^{-1} and $V_0/\tilde{A} \sim 4$.

KI: The pure electronic (0, 0) line in KI is broad (~ 7 cm^{-1}) but has no resolved fine structure or temperature-dependent width at low temperatures, just as NSP found for the infrared spectra. They inferred that there must be a high barrier to rotation about the A axis. This is also implied by the absence of stress-induced dichroism and by

the dielectric loss data of Sack and Moriarity.[15]

It is quite probable, as NSP suggest, that the nitrite ion takes an off-center position in KI. This would certainly modify the level structure of our simple rotational model. Nevertheless, a high potential barrier will cause the low-lying levels to coalesce, so that their separate transitions cannot be resolved. The only sideband will be at the librational frequency.

We note that there is a broad sideband at ~ 20 cm^{-1} in the vibronic spectra which is not observed in either the Raman or the far-infrared spectra for KI:NO_2^-. We suggest that this might be the librational sideband. It differs from KCl and KBr where the rotational frequencies were well below significant lattice frequencies, so that we could assume that the nitrite ion librates in a rigid potential. In KI, the frequencies are comparable, so that we have a resonant librational mode involing both the impurity and host ions.

As mentioned earlier, NSP assigned the infrared sidebands in the phonon gap to high-frequency librations about the *A* and *C* axes. We prefer to assign these peaks to perturbed phonons and translational modes of the nitrite ion. Certainly, in this frequency range, the librational, translational, and phonon modes will be strongly coupled.

NaBr: A low-lying peak is seen at ~ 23 cm^{-1} from the broad ν_{00} line in NaBr. We suggest that this might also be a resonant librational mode.

Rotational Raman spectra. For the one-dimensional hindered rotor the selection rule for Raman transitions is $\Delta K = 0, \pm 2, \pm 4$. This should give rise to rotational Raman lines near the Rayleigh line or to rotation vibration structure on the ν_1, ν_2, or ν_3 Raman lines.

The region close to the Rayleigh line was not examined because of the strong background of scattered light. The internal molecular lines were in a much more favorable region, but no fine structure was resolved. However, the temperature-dependent width of the ν_1 and ν_3 lines in KCl and KBr suggests that this might be due to unresolved rotational structure.

The strongly temperature-dependent behavior of the ν_3 Raman line in KBr has also been studied by Callender and Pershan.[32] They used a classical correlation-function approach to compare the temperature dependences of the widths of the ν_1 line, which has a diagonal polarizability tensor, and the ν_3 line, which has a traceless polarizability tensor. At 300 °K the NO_2^- molecule is rapidly tumbling and only the modes with nonzero trace are directly observed. As the temperature is lowered the traceless mode emerges from a broad background and becomes a well-defined line at the lowest temperature, where the correlation time for the NO_2^- rotational motion becomes appreciable. Their value of the correlation time at 100 °K, 1.4×10^{-11} sec, corresponds to a linewidth of 240 cm^{-1}, which agrees with our observation of a very broad line at 80 °K. Their spectrum at 15 °K, which shows the ν_3 line at 1276 cm^{-1} with a width of ~ 10 cm^{-1}, is in good agreement with our observation at 6 °K, which shows the line at 1274 cm^{-1} with a width of 3 cm^{-1}. Their position and width obtained for the ν_1 line also agree well with our results.

In KI, with its much larger hindering potential, the librational Raman structure should appear at higher energies. Thus it is conceivable that the main peaks in the Raman spectra of KI:NO_2^- are due to librational modes, in line with the suggestion of NSP. However, peaks of the same symmetry occur at roughly similar positions in the other alkali halides where the librator potential is very different. We reject this explanation in favor of perturbed lattice modes, as discussed previously.

The 9-cm^{-1} splitting of the ν_1 Raman line in KI might be a rotational feature, but its origin is not understood at this time.

V. SUMMARY

Raman and vibronic spectra associated with the nitrite ion have been measured at low temperatures in several alkali halides. The preferred orientation of the ion was determined from the stress-induced dichroism or splitting of the vibronic absorption lines. Rotational fine structure on these lines has been analyzed in terms of hindered rotation of the nitrite ion in a fourfold potential about ⟨100⟩ axes. Changes in rotational behavior between the ground and excited state of NO_2^- have been considered. Structure at higher frequencies in the vibronic and Raman spectra has been tentatively assigned to perturbed lattice modes and a translational mode of the nitrite ion. All these models show agreement for some features and not for others.

ACKNOWLEDGMENTS

We wish to thank I. W. Shepherd who carried out the initial Raman scattering measurements; J. B. Page, Jr., who did the lattice-dynamics calculations; V. Narayanamurti, who helped us with the intricacies of the nitrite dynamics; A. E. Hughes, who measured a far-infrared spectrum for us; and S. Othmer and J. S. Clarke, who gave computational and experimental assistance.

†Research supported by the Advanced Research Projects Agency through the Materials Science Center at Cornell, MSC Report No. 1326. Support of a Howard Hughes Fellowship is also acknowledged by one of us (A.R.E.).

*Present address: Department of Physics, University of California, Irvine, Calif. 92664.

[1]V. Narayanamurti, W. D. Seward, and R. O. Pohl, Phys. Rev. 148, 481 (1966).

[2]W. D. Seward and V. Narayanamurti, Phys. Rev. 148, 463 (1966).

[3]B. Wedding and M. V. Klein, Phys. Rev. 177, 1274 (1969); M. V. Klein, B. Wedding, and M. A. Levine, *ibid.* 180, 902 (1969).

[4]T. Timusk and W. Staude, Phys. Rev. Letters 13, 373 (1964).

[5]R. O. Pohl, Phys. Rev. Letters 8, 481 (1962); Z. Physik 176, 358 (1963).

[6]A. E. Hughes (private communication).

[7]I. W. Shepherd, A. R. Evans, and D. B. Fitchen, Phys. Letters 27A, 171 (1968); I. W. Shepherd and D. B. Fitchen, *International Symposium on Color Centers in Alkali Halides, Rome*, 1968, Abstract No. 166 (unpublished).

[8]J. S. Clarke (private communication).

[9]D. B. Fitchen, Rev. Sci. Instr. 34, 673 (1963).

[10]See, e.g., G. Herzberg, *Molecular Spectra and Molecular Structure* (Van Nostrand, Priceton, N. J., 1945), Vol. II.

[11]G. B. Carpenter, Acta Cryst. 5, 132 (1952); 8, 852 (1955).

[12]J. W. Sidman, J. Am. Chem. Soc. 79, 2669 (1957).

[13]R. Avarmaa, Izv. Akad. Nauk Est. SSR, Ser. Tekhn. i Fiz. Mat. Nauk 17, 78 (1968).

[14]R. Avarmaa and L. Rebane, Phys. Status Solidi 35, 107 (1969).

[15]H. S. Sack and C. M. Moriarty, Solid State Commun. 3, 93 (1965).

[16]M. Born and K. Huang, *Dynamical Theory of Crystal Lattices* (Oxford U. P., London, 1954), p. 203; W. Heitler, *Quantum Theory of Radiation* (Oxford U. P., London, 1954), 3rd. ed., p. 192.

[17]G. Dolling, R. A. Cowley, C. Schittenhelm, and I. M. Thorson, Phys. Rev. 147, 577 (1966).

[18]K. F. Renk, Phys. Letters 14, 281 (1965).

[19]C. D. Lytle, M. S. thesis, Cornell University, MSC Report No. 390, 1965 (unpublished); A. J. Sievers and C. D. Lytle, Phys. Letters 14, 271 (1965).

[20]G. Benedek and G. F. Nardelli, Phys. Rev. 154, 872 (1967).

[21]A. A. Maradudin, in *Solid State Physics*, edited by F. Seitz and D. Turnbull (Academic, New York, 1966), Vol. 19, p. 1.

[22]J. B. Page (private communication).

[23]U. Schroder, Solid State Commun. 4, 347 (1966); V. Nusslein and U. Schroder, Phys. Status Solidi 21, 309 (1967).

[24]A. D. B. Woods, B. N. Brockhouse, R. A. Cowley, and W. Cochran, Phys. Rev. 131, 1025 (1963); 131, 1030 (1963).

[25]W. J. L. Buyers (private communication).

[26]G. Raunio and L. Almqvist, Phys. Status Solidi 33, 209 (1969); J. R. D. Copley, R. W. MacPherson, and T. Timusk, Phys. Rev. 182, 965 (1969).

[27]For instance, M. Wagner and W. E. Bron, Phys. Rev. 139, A223 (1965).

[28]L. Pauling, Phys. Rev. 36, 430 (1930).

[29]*Tables Relating to Mathieu Functions* (Columbia U. P., New York, 1951).

[30]P. Sauer, Z. Physik 199, 280 (1967).

[31]J. S. Koehler and D. M. Dennison, Phys. Rev. 57, 1006 (1940).

[32]R. Callender and P. S. Pershan, Phys. Rev. Letters 23, 947 (1969).

PHYSICAL REVIEW B VOLUME 2, NUMBER 4 15 AUGUST 1970

Invariants of the Third-Rank Cartesian Tensor: Optical Nonlinear Susceptibilities

J. Jerphagnon*
Bell Telephone Laboratories, Murray Hill, New Jersey 07974
(Received 9 March 1970)

Optical nonlinearities in crystals are for the first time analyzed from the rotational-invariance point of view. Several previous theoretical results are discussed on the basis of the decomposition of a tensor into irreducible parts. A proportionality between the spontaneous polarization and the vector parts of the nonlinearities is established, leading to new relations for the second-harmonic generation and linear electrooptic-effect coefficients in the δ formulation.

I. INTRODUCTION

The optical properties of crystals can be described by the constitutive relations between electromagnetic field and induced polarizations. The linear properties are, for instance, determined by the second-rank tensor $\overleftrightarrow{\chi}$ relating the electric field $\vec{E}$ and the polarization $\vec{\mathcal{P}}$

$$\vec{\mathcal{P}}(\omega) = \overleftrightarrow{\chi} \cdot \vec{E}(\omega) \,. \tag{1}$$

The tensor $\overleftrightarrow{\chi}$ characterizes intrinsic properties